Macromolecules

Article

pubs.acs.org/Macromolecules

Adhesion and Wetting of Nanoparticles on Soft Surfaces

Zhen Cao,[†] Mark J. Stevens,[‡] and Andrey V. Dobrynin*,[†]

[†]Polymer Program, Institute of Materials Science and Department of Physics, University of Connecticut, Storrs, Connecticut 06269, United States

[‡]Center for Integrated Nanotechnologies, Sandia National Laboratories, Albuquerque, New Mexico 87185-1315, United States

Supporting Information

ABSTRACT: We study adhesion of spherical and cylindrical nanoparticles on soft (gel-like) substrates using a combination of the molecular dynamics simulations and theoretical calculations. The substrate deformation is obtained as a function of the gel shear modulus, nanoparticle size, surface tension of nanoparticles and substrate, and work of adhesion. It was shown recently that the classical JKR model can only be applied to describe nanoparticle adhesion on relatively stiff substrates. In this so-called adhesion regime the deformation of the substrate is determined by balancing the elastic energy of indentation and the work of adhesion between a nanoparticle and a gel. However, in the case of soft gels when substrates undergo moderate deformations the depth of the indentation produced by a nanoparticle is determined by the surface tension of the gel and the work of adhesion (the wetting regime). We present an analytical model describing crossover between adhesion and wetting regimes. In the framework of this model a crossover between different interaction regimes is controlled by a dimensionless parameter $\gamma_s(GR_p)^{-2/3}W^{-1/3}$, where γ_s and G are the surface tension and shear modulus of the gel, W is the work of adhesion between gel and nanoparticle, and R_p is the nanoparticle radius. Nanoparticle adhesion regime corresponds to small values of this parameter, $\gamma_s(GR_p)^{-2/3}W^{-1/3} \ll 1$, while the wetting regime takes place at $\gamma_s(GR_p)^{-2/3}W^{-1/3} \gg 1$. We applied our model to obtain work of adhesion between silicon substrates and silica microspheres and to obtain surface tension of silicon gels from particle indentation experiments.

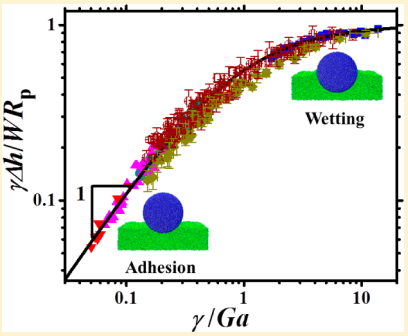

INTRODUCTION

Contact phenomena at micro- and nanoscale are important for understanding of mechanisms of adhesion and friction between surfaces,[1−9] spreading of liquid droplets on solid and elastic substrates,[10−13] adhesion and deformation of cells,[14−20] liposomes, and micro- and nanocapsules,[21−24] rippling instability of soft substrates,[11,25] for controlling resolution of molding and fabrication processes of micro- and nanoscale size features,[11,26] and AFM metrology.[27,28] This is a truly interdisciplinary area of research that has attracted attention from scientists and engineers specializing in physics, chemistry, colloidal and pharmaceutical science, tribology, biophysics, and biochemistry.

A unique feature of contact phenomena at micro- and nanoscales is that they are governed by a fine interplay between capillary and elastic forces[11,29−34]—therefore, simultaneously demonstrating features characteristic of a contact mechanics described in the framework of the Johnson−Kendall−Roberts (JKR)[1,35] or the Derjaugin, Muller, and Toporov (DMT)[36] theories and a classical Young's law for wetting of liquid on rigid substrate and Neumann's triangle for wetting on liquid interface.[10] To illustrate this point, let us consider an adhesion of a particle with size R_p on a solid substrate (see Figure 1a). In contact, a particle and substrate gain adhesion free energy (work of adhesion) W per unit area. For a contact area with radius a the total contact free energy released upon adhesion is on the order of Wa^2.[1,3] Increasing contact area particle changes its shape, resulting in increase of the elastic energy and surface free energy. We can use a Hertz expression, $U_{el} \sim Ga^5/R_p^2$,[1] to estimate elastic energy contribution due to deformation of a particle with shear modulus G. The change in the surface free energy of a particle with surface tension γ_p upon contact is $U_{surf} \sim \gamma_p a^4/R_p^2$.[10] Comparing elastic energy and surface free energy, one can show that the elastic energy provides a dominant contribution in stabilizing particle deformation when the contact radius a is larger than the elastocapillary length, γ_p/G. For elastomers with shear modulus G on the order of 10^5 Pa and surface tension γ_p = 20 mN/m, the elastocapillary length is

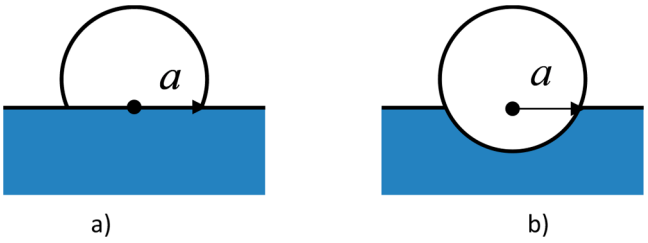

Figure 1. Schematic representation of adhesion of soft nanoparticle on rigid substrate (a) and rigid nanoparticle on soft substrate (b).

Received: February 11, 2014
Revised: April 8, 2014
Published: April 18, 2014

 © 2014 American Chemical Society

on the order of 0.2 μm. Therefore, particles made of soft elastomers will demonstrate a wetting-like behavior similar to macroscopic liquid droplets when their contact radius with a substrate is smaller than 0.2 μm. For a soft particle in adhesive contact with a solid substrate the contact radius scales as $a \approx R_p^{2/3}(W/G)^{1/3}$. In this case crossover between two regimes is governed by the dimensionless parameter $\beta \approx \gamma_p/Ga \approx \gamma_p(GR_p)^{-2/3}W^{-1/3}$.[30,31] For small values of the parameter $\beta < 1$ the equilibrium contact radius is determined by balancing elastic and adhesion energies (adhesion regime).[5,35,36] In the opposite limit $\beta > 1$ one observes a wetting-like behavior (the so-called "wetting regime") where equilibrium shape of particle is obtained by balancing variation of surface free energy and adhesion energy.[10]

It was shown recently that the classical JKR theory also breaks down for indentations produced by solid particles in soft (gel-like) substrates (see Figure 1b).[33] It was argued that the reason for this breakdown is additional contribution coming from a change in the surface free energy of the deformed substrate similar to the case of adhesion of soft nanoparticles discussed above. To prove that this is indeed the case in this paper, we use a combination of the molecular dynamics simulations and analytical calculations to study interactions between solid spherical and cylindrical nanoparticles and gels (soft substrates) (see Figure 2). In particular we establish how

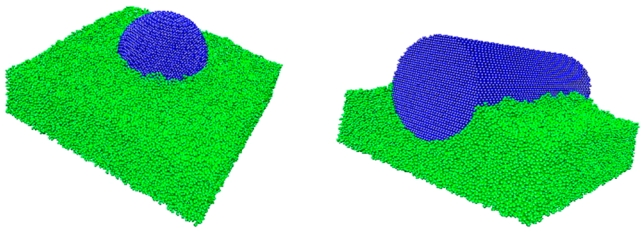

Figure 2. Snapshot of the simulation box with elastic substrate shown in green color and a spherical (left) and cylindrical (right) nanoparticle shown in blue.

nanoparticle/substrate adhesion energy W, substrate shear modulus G, surface tension γ_s, and nanoparticle size R_p influence depth of nanoparticle indentation and size of the contact. This allows us to show that for adhesion of hard nanoparticles on soft substrate there are two different substrate deformation regimes. We applied our approach to obtain work of adhesion between silicon gels and glass particles and surface tension of silicon gels from indentation experiments.[33]

RESULTS AND DISCUSSION

We have performed molecular dynamics simulations[37] of adhesion of spherical and cylindrical nanoparticles on gel substrates with thickness H (see Figure 2). In our simulations we used a coarse-grained representation of nanoparticles and gel substrates. In this representation nanoparticles were made of beads with diameter σ arranged into hexagonal closed-packed (HCP) lattice. Substrates have a gel-like structure and consist of randomly cross-linked bead−spring chains. The gel elasticity was controlled by changing cross-linking density. The interactions between all beads in a system were modeled by truncated and shifted Lennard-Jones potential with the interaction parameter ϵ_{LJ} and value of the cut off radius r_{cut}. The connectivity of beads into polymer chains and cross-links between polymer chains and bonds holding nanoparticles together were modeled by the FENE potential.[38] The elastic substrate with thickness H was placed on top of a solid substrate which is modeled by an external 3−9 potential with the value of the interaction parameter ϵ_w. The actual parameters for potentials, their explicit form, and simulation details are given in the Supporting Information. All simulations were performed using LAMMPS.[39]

Spherical Nanoparticles. We first discuss our results for adhesion of spherical nanoparticles due to interactions with a substrate. Figure 3 shows variation of the depth of indentation produced by a rigid nanoparticle in a gel as a function of the gel shear modulus, G, and nanoparticle radius, R_p. The values of the substrate shear modulus were obtained from simulations of the 3-d networks with the same polymer and cross-linking densities.[29] In the case of strongly cross-linked substrates, that corresponds to larger values of the shear modulus, adhesion of nanoparticles leads only to shallow indentations. In this case the effective contact angle θ is larger than 100°, and substrate could be considered as particle-phobic for all nanoparticles independent of their sizes. The indentation depth increases with increasing nanoparticle size. By increasing nanoparticle size, one increases the contact area between nanoparticle and substrate, which in turn increases the total strength of adhesion between a nanoparticle and a substrate. Indentation depth also increases with decreasing substrate shear modulus. Decrease in the substrate shear modulus lowers the elastic energy penalty for creation of indentation. Another interesting feature of the adhesion of nanoparticle on soft substrate as observed in Figure 3 is the existence of the ridge. The ridge height increases with decreasing substrate shear modulus. Analysis of the indentation shape variation with system parameters shows that there exists an interesting interplay between interfacial and elastic energies in determining the equilibrium shape of the contact between nanoparticle and substrate.

In order to quantify the effect of adhesion, elastic, and capillary forces in nanoparticle/gel systems, we will approximate an indentation produced by nanoparticle in a gel by a spherical cup-like indentation shown in Figure 4 and use the approach developed in ref 30. In this approximation one neglects the contribution from the ridge (see Figure 3). Note that in the framework of this approach we will not be able to reproduce a correct value of the contact angle θ which requires a solution for gel height profile outside the contact area.[12] For a spherical nanoparticle geometrical constraint for spherical cup indentation the indentation depth Δh and radius of indentation a are not independent parameters and are related through the following equation: $a^2 = 2R_p\Delta h - \Delta h^2$. Taking this into account, we can evaluate the change in the system surface free energy caused by indentation (see Supporting Information for derivation details)

$$\Delta F_{surf}(\Delta h) = -2\pi W R_p \Delta h + \pi\gamma_s \Delta h^2 \quad (1)$$

where W is the work of adhesion per unit area, $W = \gamma_s + \gamma_p - \gamma_{sp}$, between substrate (s) and nanoparticle (p), and γ_s is the surface tension of the gel. The stored elastic energy of indentation in the case of small deformations, $\Delta h/R_p \ll 1$, is estimated as

$$U_{elas}(\Delta h) \approx CKR_p^{1/2}\Delta h^{5/2} \quad (2)$$

where C is a numerical constant which value depends on the model used to describe stress distribution.[1,30,34,40] Here we will

dx.doi.org/10.1021/ma500317q | Macromolecules 2014, 47, 3203−3209

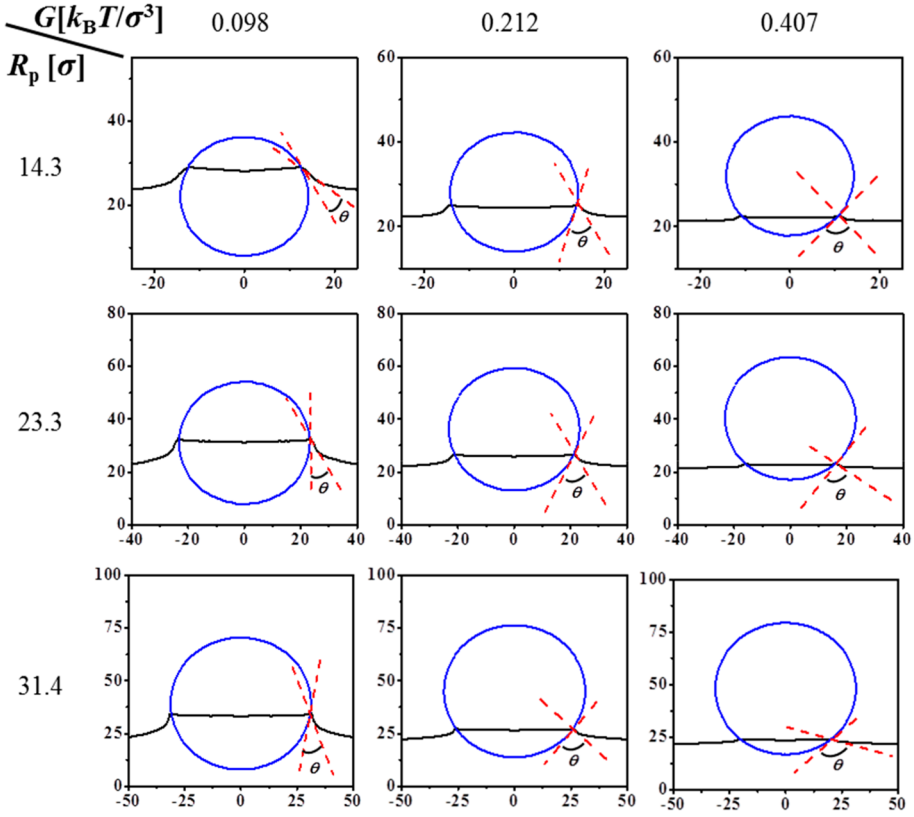

Figure 3. Average shape of indentation and contact angle θ produced by a spherical nanoparticle with size R_p on substrates with shear modulus G.

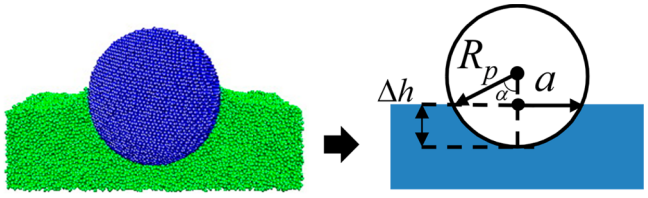

Figure 4. Schematic representation of the substrate indentation produced by a nanoparticle with radius R_p used for derivation of the indentation free energy.

consider this numerical constant as an adjustable parameter. $K = 2G/(1 - \nu)$ is the rigidity of the substrate with shear modulus G and the Poisson ratio ν. For rubbery substrates with $\nu = 1/2$ the substrate rigidity $K = 4G$. Note that we can neglect a finite thickness of the gel up to indentation depths such that $a/H \leq 1$ and approximate a substrate by an infinite half-space.[40] Combining elastic and surface contributions (eqs 1 and 2), we arrive at

$$\Delta F(\Delta h) \approx -2\pi W R_p \Delta h + \pi \gamma_s \Delta h^2 + C K R_p^{1/2} \Delta h^{5/2} \quad (3)$$

It follows from eq 3 that the release of the adhesion energy (the first term in the right-hand side of eq 3) which is responsible for deepening the indentation in the substrate can be opposed either by the surface free energy (the second term in eq 3) or by the elastic energy (the last term in eq 3). In order to obtain a general expression for dependence of the indentation depth, Δh, as a function of the system parameters, we have to optimize the total expression for the system free energy eq 3 with respect to Δh

$$0 \approx -2\pi W R_p + 2\pi \gamma_s \Delta h + \frac{5}{2} C K R_p^{1/2} \Delta h^{3/2} \quad (4)$$

The classical adhesion scaling dependence of the indentation depth Δh on the work of adhesion W is obtained by balancing the adhesion and elastic energy terms:

$$\Delta h \propto R_p (W/G R_p)^{2/3} \quad (5)$$

We will refer to this regime as the *adhesion regime*. Using relation between contact radius a and indentation depth Δh for small deformations, $a \approx (\Delta h R_p)^{1/2}$, we can express Δh in terms of a ratio of W/G to the contact radius a by substituting $R_p^{1/2} \Delta h^{3/2} \approx \Delta h a$ in eq 4

$$\Delta h / R_p \propto W/Ga \quad (6)$$

However, when the contact radius a becomes smaller than elastocapillary length γ_s/G, the equilibrium indentation depth is obtained by balancing adhesion and surface free energy terms resulting in the expression

$$\Delta h / R_p \approx W/\gamma_s \quad (7)$$

We call this regime the *wetting regime*. We can write a general solution of eq 4 for the depth of indentation Δh as a function of the contact radius a as follows

$$\frac{\gamma_s}{W} \frac{\Delta h}{R_p} \approx \left(1 + C_a \frac{Ga}{\gamma_s}\right)^{-1} \quad (8)$$

where a numerical constant C_a should be considered as a fitting parameter which value can be obtained by fitting the simulation data.

dx.doi.org/10.1021/ma500317q | *Macromolecules* 2014, 47, 3203−3209

To illustrate the existence of two different scaling regimes in substrate deformation, Figure 5 shows the dependence of the

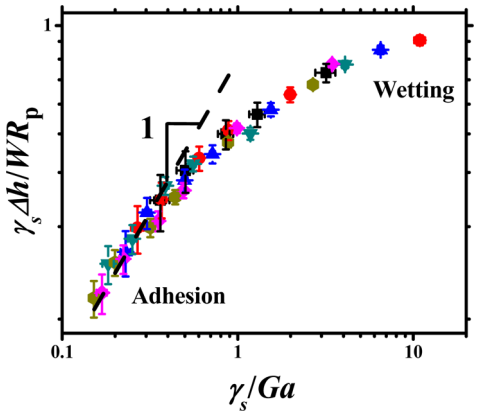

Figure 5. Dependence of the reduced nanoparticle indentation depth, $\gamma_s\Delta h/WR_p$, on the ratio of the elastocapillary length to indentation radius, γ_s/Ga, for nanoparticles with different sizes R_p: 9.8σ (black squares), 14.3σ (red cycles), 17.9σ (blue triangles), 23.2σ (cyan inverted triangles), 27.7σ (magenta rhombs), and 31.4σ (green hexagons).

reduced indentation depth $\gamma_s\Delta h/WR_p$ on the ratio of the elastocapillary length to indentation radius, γ_s/Ga. For this plot the values of the work of adhesion, W, surface tension of gel, γ_s, and gel shear modulus, G, were calculated in separate simulations (see Supporting Information and refs 29 and 30 for details). It follows from this figure that there are two different regimes in dependence of $\Delta h/R_p$ on the system parameters. At small values of the parameter γ_s/Ga the indentation depth demonstrates a linear dependence on the ratio of the elastocapillary length to the contact radius as expected from eq 6. However, when the ratio γ_s/Ga exceeds unity, we begin to observe a deviation from linear scaling dependence. This indicates that the surface free energy term (see eqs 3 and 4) begins to influence interactions between nanoparticle and substrate.

Figure 5 shows a very good collapse of our simulation data for which we know system parameters such as W, G, and γ_s. Thus, we can use this result and fit simulation and experimental data to obtain experimental values for W and γ_s from indentation depth Δh and a contact radius, a. To improve accuracy of the procedure, we have added previous simulation results for adhesion of soft nanoparticles on rigid (undeformable) substrates.[30] Note that these two examples (adhesion of soft nanoparticles on rigid substrate and rigid nanoparticles on soft substrates) represent two limiting cases of the general adhesion problem between two objects with arbitrary radii of curvature and elastic properties.[1] In addition the surface free energy terms have identical functional form in both cases (see eq 1 and ref 30). We first fit all simulation data to obtain value of the numerical constant $C_a = 0.816$. After that we fit each experimental data set for adhesion of glass spheres on silicon substrates provided by Dufresne's group[33] and obtained work of adhesion between glass particles and silicon gels and gel surface tension. The fitting parameters are summarized in Table 1. Note that for the samples with the largest value of the shear modulus, $G = 167$ kPa, we have only used work of adhesion, W, as a fitting parameter and fixed value of the surface tension, γ_s, to that obtained for samples with $G = 83.3$ kPa. For this data set the contribution to substrate deformation from surface free

Table 1. Work of Adhesion and Surface Tension for Silicon/Glass Systems

	G (kPa)			
	1.0	28.3	83.3	167
fitting parameters	γ_s, W	γ_s, W	γ_s, W	W
W (mN/m)	68.5 ± 3.0	77.6 ± 3.4	75.9 ± 4.7	66.8 ± 1.7
γ_s (mN/m)	46.9 ± 2.3	62 ± 11	65 ± 27	65

energy is too small to be able to resolve it. The results of this fitting procedure and simulation data are combined in Figure 6. It is important to point out that in the case of adhesion of soft nanoparticle on rigid substrate in eq 8 we have to use nanoparticle surface tension γ_p (see ref 30).

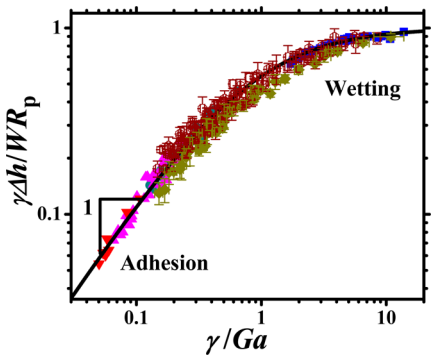

Figure 6. Dependence of the reduced substrate indentation or nanoparticle deformation, $\gamma\Delta h/WR_p$, on the ratio of the elastocapillary length to contact radius, γ/Ga. The solid line corresponds to eq 8 with numerical constant $C_a = 0.816$. Simulation results for adhesion of rigid nanoparticles on soft substrates are shown by filled rhombs and for adhesion of soft nanoparticles on solid substrates are shown by open hexagons. Experimental data for adhesion of glass particles on silicon substrates with different values of the shear modulus G are shown as 1 kPa (blue squares), 28.3 kPa (cyan circles), 83.3 kPa (magenta triangles), and 167 kPa (inverted red triangles).

We can also obtain dependence of the indentation depth Δh on the system parameters by solving eq 4. Following the approach developed in ref 30, we introduce dimensionless variables $y^2 = (\Delta h/2R_pA)(KR_p/W)^{2/3}$ and $\beta = B(\gamma_s^{3/2}/KR_pW^{1/2})^{2/3}$ (where $A = (\sqrt{2\pi}/5C)^{2/3}$ and $B = 2(\sqrt{2\pi}/5C)^{2/3}$ are numerical coefficients) and can reduce eq 4 to a simple cubic equation

$$0 = -1 + \beta y^2 + y^3 \tag{9}$$

The deformation of a gel by a spherical nanoparticle is described by a positive root of this equation

$$\frac{\Delta h}{2R_p} = A\left(\frac{W}{KR_p}\right)^{2/3}\left(\sqrt[3]{r+\sqrt{q^3+r^2}} + \sqrt[3]{r-\sqrt{q^3+r^2}} - \frac{\beta}{3}\right)^2 \tag{10}$$

where

$$r = \frac{1}{2} - \left(\frac{\beta}{3}\right)^3 \quad \text{and} \quad q = -\left(\frac{\beta}{3}\right)^2 \tag{11}$$

The actual values of the parameters A and B are model dependent, and we will consider them as adjustable parameters to fit our simulation data. One can also express reduced parameters in terms of the shear modulus G. In this case the

dx.doi.org/10.1021/ma500317q | Macromolecules 2014, 47, 3203−3209

values of the numerical coefficients are $A_G = A((1 - \nu)/2)^{2/3}$ and $B_G = 2A_G$. Analysis of the solution eq 10 shows that we recover eq 5 in the limit of small values of the parameter $\beta \approx \gamma_s(GR_p)^{-2/3}W^{-1/3}$. This corresponds to the adhesion regime. However, in the interval of large values of this parameter, $\beta \gg 1$, which is the case for weakly cross-linked substrates, the indentation depth is given by eq 7. In this interval of parameters there is a meniscus formation around nanoparticle (see Figure 3).

In Figure 7, we plotted dependence of the reduced particle deformation $(GR_p/W)^{2/3}\Delta h/2R_p$ on the value of the parameter $\gamma(GR_p)^{-2/3}W^{-1/3}$ for spherical nanoparticle indentations together with experimental data by Style et al.[33] and simulation data for adhesion of gel nanoparticles on rigid substrates.[30] The solid line represents a best fit to eq 10 with the values of the fitting parameters $A_G = 0.416$ and $B_G = 0.798$. All data sets have collapsed into one universal plot and demonstrate a very good agreement between simulation and experimental data. This confirms validity of our approach in describing adhesion of nanoparticles on substrates with different elastic properties. It is important to point out that at small values of the parameter $\gamma(GR_p)^{-2/3}W^{-1/3}$ corresponding to adhesion regime we see a larger scattering of the data. In this interval of parameters particles produce a very small indentation; therefore, a small error in determination of the indentation depth could result in a large data scattering since the values are obtained by division of two small numbers.

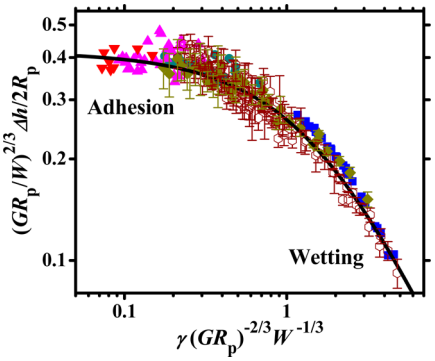

Figure 7. Dependence of the reduced substrate indentation or nanoparticle deformation on the value of the parameter $\gamma(GR_p)^{-2/3}W^{-1/3}$ for substrates and nanoparticles with different cross-linking densities, different strengths of the substrate−polymer interactions, and different nanoparticle sizes. Solid line corresponds to eq 10 with values of the fitting parameters $A_G = 0.416$ and $B_G = 0.798$. Notations are the same as in Figure 6.

Cylindrical Nanoparticles. Indentations produced by cylindrical nanoparticles in soft substrates demonstrate features similar to those observed for spherical nanoparticles. This is illustrated in Figure 8 which shows how shape of indentation produced by cylindrical nanoparticle and contact angle changes with cylinder radius, R_p, and shear modulus, G, of the substrate. Below we will show that the scaling dependence of the indentation depth and crossover between the adhesion and wetting regimes are governed by a similar dimensional group as in the case of adhesion of spherical nanoparticle. For adhesion of cylindrical nanoparticle it is useful to describe indentation depth $\Delta h \approx R_p\alpha^2/2$ and contact length $a \approx R_p\alpha$ in terms of angle α (see Figure 4). The change in the free energy of the system per unit length of the cylindrical nanoparticle as a function of the angle α is written as follows

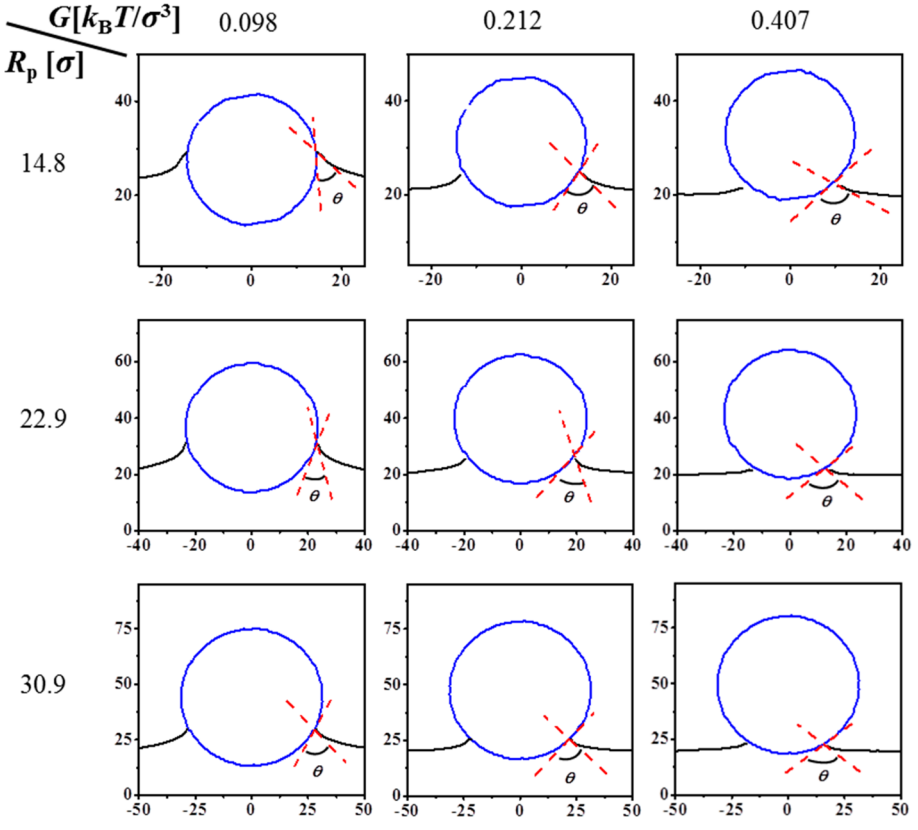

Figure 8. Average shape of indentation and contact angle θ induced by a cylindrical nanoparticle with size R_p on substrates with shear modulus G.

dx.doi.org/10.1021/ma500317q | Macromolecules 2014, 47, 3203−3209

$$\Delta F(\alpha) \approx -2WR_p\alpha + \frac{1}{3}\gamma_s R_p\alpha^3 + \frac{1}{4}CKR_p{}^2\alpha^4 \quad (12)$$

where C is a numerical constant for the elastic energy of the cylindrical indenter. The exact expression for the elastic energy can be obtained by integrating the stress distribution and displacement within the contact length.[1,30] A scaling expression of the stored elastic energy per unit length produced by a cylindrical nanoparticle can be estimated by using the following simple arguments. For indentation depth Δh the typical value of the restoring stress σ_{zz} in the contact area is on the order of $G\Delta h/a$. This stress distributed over a contact length $2a$ produces a restoring force per unit length on the order of $\sigma_{zz}a$. The stored elastic energy is on the order of work required to maintain indentation Δh with a force equal to a restoring force $\sigma_{zz}a$. This results in elastic energy per unit length to be on the order of $U_{elast} \propto \sigma_{zz}a\Delta h \approx G\Delta h^2$. The derivation of the surface free energy terms is given in the Supporting Information.

The equilibrium angle α is obtained by minimizing the free energy eq 12.

$$0 \approx -2W + \gamma_s\alpha^2 + CKR_p\alpha^3 \quad (13)$$

It follows from eq 13 that there are two different regimes for interaction of the cylindrical nanoparticle with gel. The adhesion scaling dependence of the indentation depth Δh on the work of adhesion W is obtained by balancing the adhesion and elastic energy terms:

$$\Delta h \approx R_p\alpha^2 \approx R_p(W/GR_p)^{2/3} \quad (14)$$

Using the relation between a contact length a and indentation depth Δh for small deformations, we can express Δh as a ratio of W/G and the contact length $a \approx R_p\alpha$ and recover eq 5. In the other limit when $\gamma_s/Ga \gg 1$ to obtain equilibrium indentation depth, Δh, we have to balance adhesion and surface free energy terms in eq 13. This results in expression similar to eq 7. In Figure 9 we show dependence of the reduced indentation depth $\gamma_s\Delta h/WR_p$ on the ratio of the elastocapillary length to indentation length, γ_s/Ga. As one can see, the simulation results demonstrate a very nice collapse in both deformation regimes. It is important to point out that indentations produced by cylindrical nanoparticles demonstrate similar scaling dependences on the system parameters as those produced by spherical nanoparticles.

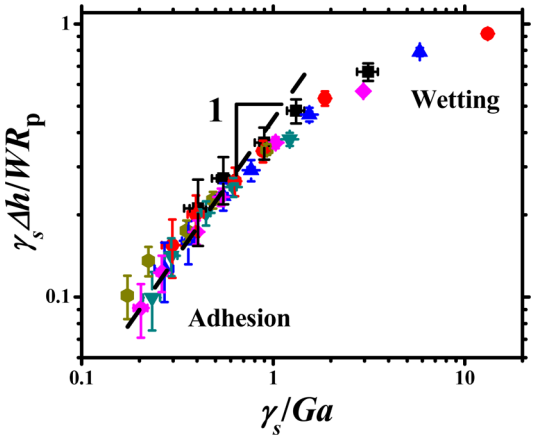

Figure 9. Dependence of the reduced indentation depth, $\gamma_s\Delta h/WR_p$, on the ratio of the elastocapillary length to indentation length, γ_s/Ga, produced by cylindrical nanoparticles with size R_p: 9.8σ (black squares), 14.3σ (red cycles), 17.9σ (blue triangles), 23.2σ (cyan inverted triangles), 27.7σ (magenta rhombs), and 31.4σ (green hexagons).

As in the case of spherical nanoparticles, we can introduce dimensionless variables $y = A_{cyl}\alpha(GR_p/W)^{1/3}$ and $\beta_{cyl} = B_{cyl}(\gamma_s{}^{3/2}/GR_pW^{1/2})^{2/3}$ (where $A_{cyl} = (C/(1-\nu))^{1/3}$ and $B_{cyl} = 1/(2A_{cyl}{}^2)$ are numerical coefficients) and reduce eq 13 to a cubic equation

$$0 = -1 + \beta_{cyl}y^2 + y^3 \quad (15)$$

Solving this equation, we obtain for indentation depth

$$\frac{\Delta h}{R_p} = \frac{1}{2A_{cyl}{}^{2/3}}\left(\frac{W}{GR_p}\right)^{2/3}\left(\sqrt[3]{r+\sqrt{q^3+r^2}} + \sqrt[3]{r-\sqrt{q^3+r^2}} - \frac{\beta_{cyl}}{3}\right)^2 \quad (16)$$

where in expressions for r and q (see eqs 10) we have to substitute β by β_{cyl}. Using these new reduced variables, we can collapse our simulation data for cylindrical nanoparticle as shown in Figure 10.

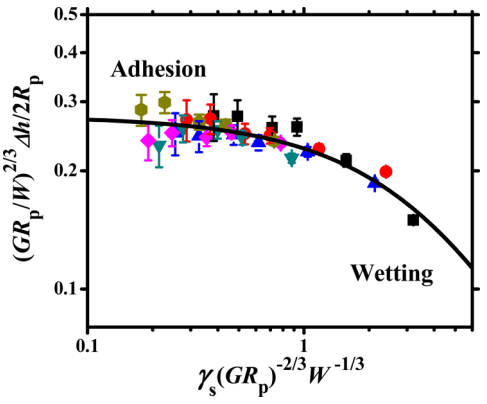

Figure 10. Dependence of the reduced substrate indentation depth produced by a cylindrical nanoparticle on the value of the parameter $\gamma_s(GR_p)^{-2/3}/W^{-1/3}$ for substrates with different values of the shear modulus and different nanoparticle sizes. Notations are the same as in Figure 9. Solid line corresponds to eq 16 with values of fitting parameters $A_{cyl} = 0.864$ and $B_{cyl} = 0.299$.

CONCLUSIONS

To summarize, we have used a combination of the molecular dynamics simulations and analytical calculations to study interaction of rigid spherical and cylindrical nanoparticles with gel substrates. Our analysis shows that interaction of nanoparticles with substrate is a result of interplay between elastic, adhesion, and surface energies. Crossover between different gel deformation regimes is governed by a dimensionless parameter $\gamma_s(GR_p)^{-2/3}W^{-1/3}$. In the interval of system parameters for which this parameter $\gamma_s(GR_p)^{-2/3}W^{-1/3}$ is small, the indentation depth produced by nanoparticle in a gel is determined by balancing the substrate elastic energy and work of adhesion between nanoparticle and substrate (adhesion regime). However, in the opposite limit when the parameter $\gamma_s(GR_p)^{-2/3}W^{-1/3}$ is large, the indentation depth is controlled by balance of the interfacial free energy and work of adhesion (wetting regime). This universal behavior of nanoparticle interaction with gel does not depend on the nanoparticle geometry, and it is observed for spherical and cylindrical nanoparticles. We have applied our model of nanoparticle

dx.doi.org/10.1021/ma500317q | Macromolecules 2014, 47, 3203−3209

adhesion to obtain work of adhesion between silicon substrates and glass spheres and surface tension of silicon substrates as a function of substrate elastic properties.[33] This approach could become a valuable technique for obtaining work of adhesion and surface tension of elastomers from indentation experiments.

■ ASSOCIATED CONTENT

Supporting Information

Description of simulations details, calculations of the work of adhesion, gel surface tension, and derivation of the surface free energy terms in eqs 1 and 12. This material is available free of charge via the Internet at http://pubs.acs.org.

■ AUTHOR INFORMATION

Corresponding Author

*E-mail avd@ims.uconn.edu (A.V.D.).

Notes

The authors declare no competing financial interest.

■ ACKNOWLEDGMENTS

The authors thank Prof. Eric Dufresne and Dr. Robert Style for providing original experimental data sets. This work was supported by the National Science Foundation under Grant DMR-1004576. This work was performed at the U.S. Department of Energy, Center for Integrated Nanotechnologies, at Los Alamos National Laboratory (Contract DE-AC52-06NA25396) and Sandia National Laboratories. Sandia is a multiprogram laboratory operated by Sandia Corporation, a Lockheed Martin Company, for the United States Department of Energy under Contract DE-AC04-94AL85000.

■ REFERENCES

(1) Johnson, K. L. *Contact Mechanics*, 9th ed.; Cambridge University Press: New York, 2003.
(2) Persson, B. N. J. *Sliding Friction. Physical Principles and Applications*; Springer: Berlin, 2000.
(3) Johnson, K. L. *Tribology Int.* **1998**, *31*, 413.
(4) Gerberich, W. W.; Cordill, M. J. *Rep. Prog. Phys.* **2006**, *69*, 2157.
(5) Barthel, E. *J. Phys. D: Appl. Phys.* **2008**, *41*, 163001.
(6) Crosby, A. J.; Shull, K. R. *J. Polym. Sci., Part B: Polym. Phys.* **1999**, *37*, 3455.
(7) Mo, Y. F.; Turner, K. T.; Szlufarska, I. *Nature* **2009**, *457*, 1116.
(8) Szlufarska, I.; Chandross, M.; Carpick, R. W. *J. Phys. D: Appl. Phys.* **2008**, *41*, 39.
(9) Maugis, D. *J. Colloid Interface Sci.* **1992**, *150*, 243.
(10) de Gennes, P.-G.; Brochard-Wyart, F.; Quere, D. *Capillarity and Wetting Phenomena*; Springer: New York, 2002.
(11) Roman, B.; Bico, J. *J. Phys.: Condens. Matter* **2010**, *22*, 16.
(12) Style, R. W.; Dufresne, E. R. *Soft Matter* **2012**, *8*, 7177.
(13) Style, R. W.; Boltyanskiy, R.; Che, Y.; Wettlaufer, J. S.; Wilen, L. A.; Dufresne, E. R. *Phys. Rev. Lett.* **2013**, *110*, 066103.
(14) Evans, E. *Annu. Rev. Biophys. Biomol. Struct.* **2001**, *30*, 105.
(15) Evans, E. A.; Calderwood, D. A. *Science* **2007**, *316*, 1148.
(16) Schmitz, J.; Gottschalk, K. E. *Soft Matter* **2008**, *4*, 1373.
(17) Trepat, X.; Lenormand, G.; Fredberg, J. J. *Soft Matter* **2008**, *4*, 1750.
(18) Leckband, D. *Cell. Mol. Bioeng.* **2008**, *1*, 312.
(19) Chu, Y. S.; Dufour, S.; Thiery, J. P.; Perez, E.; Pincet, F. *Phys. Rev. Lett.* **2005**, *94*, 028102.
(20) Discher, D. E.; Jammey, P.; Wang, Y.-L. *Science* **2005**, *310*, 1139.
(21) Shull, K. R. *Mater. Sci. Eng., R* **2002**, *36*, 1.
(22) Shull, K. R. *J. Polym. Sci., Part B: Polym. Phys.* **2006**, *44*, 3436.
(23) Fery, A.; Dubreuil, F.; Mohwald, H. *New J. Phys.* **2004**, *6*, 18.
(24) Liu, K. K. *J. Phys. D: Appl. Phys.* **2006**, *39*, R189.
(25) Huang, J.; Davidovich, B.; Santangelo, C.; Russel, T. P.; Menon, N. *Phys. Rev. Lett.* **2010**, *105*, 038302.
(26) Gates, B. D.; Xu, Q. B.; Stewart, M.; Ryan, D.; Willson, C. G.; Whitesides, G. M. *Chem. Rev.* **2005**, *105*, 1171.
(27) Franz, C. M.; Puech, P. H. *Cell. Mol. Bioeng.* **2008**, *1*, 289.
(28) Ptak, A.; Kappl, M.; Moreno-Flores, S.; Gojzewski, H.; Butt, H. J. *Langmuir* **2009**, *25*, 256.
(29) Carrillo, J. M. Y.; Dobrynin, A. V. *Langmuir* **2009**, *25*, 13244.
(30) Carrillo, J. M. Y.; Raphael, E.; Dobrynin, A. V. *Langmuir* **2010**, *26*, 12973.
(31) Carrillo, J. M. Y.; Dobrynin, A. V. *Langmuir* **2012**, *28*, 10881.
(32) Carrillo, J. M. Y.; Dobrynin, A. V. *J. Chem. Phys.* **2012**, *137*, 214902.
(33) Style, R. W.; Hyland, C.; Boltyanskiy, R.; Wettlaufer, J. S.; Dufresne, E. R. *Nat. Commun.* **2013**, *4*, 2728.
(34) Salez, T.; Benzaquen, M.; Raphael, E. *Soft Matter* **2013**, *9*, 10699.
(35) Johnson, K. L.; Kendall, K.; Roberts, A. D. *Proc. R. Soc. London A* **1971**, *324*, 301.
(36) Derjaguin, B. V.; Muller, V. M.; Toporov, Y. P. *J. Colloid Interface Sci.* **1975**, *53*, 314.
(37) Frenkel, D.; Smit, B. *Understanding Molecular Simulations*; Academic Press: New York, 2002.
(38) Kremer, K.; Grest, G. S. *J. Chem. Phys.* **1990**, *92*, 5057.
(39) Plimpton, S. *J. Comput. Phys.* **1995**, *117*, 1.
(40) Johnson, K. L.; Sridhar, I. *J. Phys. D: Appl. Phys.* **2001**, *34*, 683.